# Theoretical characterization of the high-pressure phases of $PbF_2$

Aurora Costales,* M. A. Blanco,† and Ravindra Pandey
*Department of Physics, Michigan Technological University, Houghton, Michigan, 49931*

J. M. Recio
*Departamento de Química Física y Analítica, Universidad de Oviedo, 33006 Oviedo, Spain*
(Received 27 October 1999)

*Ab initio* perturbed ion calculations were performed for the cubic, orthorhombic, hexagonal, and monoclinic phases of $PbF_2$. A complete characterization of these phases was achieved in terms of the potential energy surfaces, the equations of state, and the phase-transition pressures. Thermal effects were included via a quasiharmonic nonempirical Debye model. The internal parameters of the unit cell of each phase were reoptimized at each volume to generate the energy surface. The calculated results are in good agreement with the experimental data available for the cubic and orthorhombic phases. The results predict the hexagonal phase to be the high-pressure post-cotunnite structure for $PbF_2$, since the monoclinic phase is seen to collapse into the hexagonal phase during the optimization at high pressures.

## I. INTRODUCTION

Lead fluoride in its cubic, native form, is a technologically important scintillating material,[1,2] and is also known to exhibit superionic conductivity.[3] Upon increasing pressure, it goes through an irreversible transition to an orthorhombic phase in which it loses these properties.[1,4] This phase is metastable at ambient conditions, and has been well characterized experimentally.[5] However, at higher pressures, the metastable phase transforms to a phase which is yet to be characterized fully.[6,7]

The low-pressure $PbF_2$ polymorphs are known as $\alpha$-$PbF_2$ and $\beta$-$PbF_2$. The $\beta$ structure is the most stable in ambient conditions, and is a cubic, fluorite-type (C1) crystal. On the other hand, the orthorhombic $\alpha$ polymorph is stable at higher pressure and low temperature, with $\alpha$-$PbCl_2$-like (cotunnite, C23) structure. $PbF_2$ undergoes a phase transition at about 0.4 GPa from C1 to C23, and reverses back to C1 at higher temperatures. The C23 phase is metastable at zero pressure for $T<610$ K.[8] Recently, there has been some experimental evidence of a new phase of $PbF_2$. Podsiadlo and Matuszewski[6] have reported a phase of hexagonal symmetry, tentatively assigned as P6, with lattice parameters of $a=10.2746(6)$ and $c=7.970(5)$ Å. On the other hand, Lorenzana et al.[7] have conducted Raman experiments showing a transition from the C23 phase at around 15 GPa. The observed Raman peaks of the high-pressure structure of $PbF_2$ cannot be explained by assuming hexagonal symmetry. These peaks, however, can also not be assigned to a monoclinic phase unambiguously. These authors have also done first-principles calculations where they find a hexagonal phase, $Ni_2In$-like ($B8_b$), to be more stable than the C23 phase at 16.4 GPa. Despite this fact, they use their Raman measurements in favor of a monoclinic structure, although, due to limited computational resources, they have not done any calculation in the monoclinic phase.

It is known that divalent metal halides such as $BaF_2$, $BaCl_2$, $PbCl_2$, and $SnCl_2$ occur in the cotunnite structure, either at ambient conditions or at moderately high pressures. They also undergo a phase transition from the C23 phase to a high-coordinated phase. In the case of lead and tin chlorides (and presumably in $BaCl_2$), Léger *et al.* have characterized the post-cotunnite phase within the $P2_1/c$ (monoclinic) symmetry,[9,10] with coordination of 10. The same authors have also characterized the high-pressure phase of $BaF_2$ to be that of $Ni_2In$,[11] with coordination of 11, the highest found in ionic materials.

In this paper, we will consider all the different phases, either those experimentally detected or those proposed by analogy with other compounds, with an aim to fully characterize ambient and high-pressure phases of lead fluoride. We will use the *ab initio* perturbed ion (*ai*PI) method[12–14] which has been proven to be successful in studying the phase transition in ionic and semiionic materials. We will compute the equation of state for each phase of $PbF_2$, as well as the transition pressures between them, comparing, when possible, with experimental data.

## II. COMPUTATIONAL DETAILS

The *ai*PI method is a quantum-mechanical method that solves the Hartree-Fock (HF) equations of a solid in a localized Fock space by partitioning the crystal wave function into local, weakly overlapping group functions, each containing a number of electrons but a single nucleus. The method brings together ideas from the theory of electronic separability of McWeeny and Huzinaga, and from the theory of localizing potentials of Adams and Gilbert, to produce a well founded and very efficient treatment for ionic materials (see Ref. 15 and references therein). The *ai*PI method has been successfully applied to the description of a variety of electronic, energetic, and structural properties of ionic crystals, including halides, oxides, and sulfides.[16,17] The *ai*PI calculations in the present work have been done using the Koga *et al.* Slater-type (STO) all-electron basis sets, the negative F basis set for the fluoride ion,[18] and the neutral Pb basis set[19] for the lead ion, after removal of the outermost *p* exponent and reoptimization of the remaining valence exponents. The

 

correlation energy has been estimated using the Lee-Yang-Parr functional.[20]

In order to generate thermodynamic data at finite temperatures and pressures, we have used a quasiharmonic Debye-like model in which the Debye temperature $\Theta$ depends only on volume through the static bulk modulus as $\Theta = CV^{1/6}[B_{st}(V)]^{1/2}$, where $C$ is a constant which depends on the molecular mass and Poisson ratio.[21] This approach allows us to write all thermodynamic quantities in terms of the $E(V)$ curve, so that we only need to optimize the energy with respect to all internal variables for each volume. Using the $E(V)$ curve and its derivatives, we obtain the equation of state of a given phase by minimizing the nonequilibrium Gibbs energy for each $P$ and $T$ with respect to the volume, $G^*(T,P;V) = E(V) + PV + F_{vib}(T,\Theta(V))$, $F_{vib}$ being the Helmholtz vibrational energy within the Debye model. Other thermodynamic properties can be computed by substituting the equilibrium volume for each $P$ and $T$. In order to obtain thermodynamic properties at the phase transition, we impose the equilibrium condition of an equal Gibbs function for the two phases considered, and so we construct the $P(T)$ equilibrium line of the phase diagram.

### III. RESULTS AND DISCUSSION

The $\beta$-$PbF_2$ phase has only one free parameter, namely the length of the cell $a$, since all ions are occupying fixed special positions. Thus, each point in the $E(V)$ curve requires a single calculation with no optimization of internal parameters. On the other hand, the $\alpha$-$PbF_2$ phase has nine free parameters. The structure belongs to the orthorhombic crystallographic system (space group $Pnma$) with $a \neq b \neq c$ variables. Also, the three ions (Pb and two different F ions) are in the $4c$ Wyckoff position ($C_s$ symmetry), with free internal $x$ and $z$ coordinates. The optimized parameters of this orthorhombic C23 phase were obtained by a downhill simplex method[22] and are presented in Fig. 1. All of them vary smoothly with decreasing volumes, but show an abrupt change at about 255 bohr$^3$/molecule. For smaller volumes, the internal parameters and $b/c$ adopt constant values as shown in Fig. 1. This has suggested that there must be a higher symmetry polymorph which becomes relatively more stable than the C23 phase.

We have identified the high-symmetry polymorph as the hexagonal $B8_b$ phase, with space group $P6_3/mmc$. The $Pb^{+2}$ ion goes to position $2d$ ($D_{3h}$), while the $F^-$ ions go to $2a$ ($D_{3d}$) and $2c$ ($D_{3h}$), with a unit cell that is half the size of the orthorhombic one. This hexagonal phase has only two free parameters, $a'$ and $c'$, and its $E(V)$ curve therefore requires only a monodimensional optimization of $a'/c'$. It is important to stress the fact that this phase lies within the 9-parameter space of the C23 phase, with the internal coordinates and $b/c$ fixed to the values shown in Fig. 1. The $a$ axis of the C23 phase corresponds to the inequivalent hexagonal axis $c'$. Using the $c = \sqrt{3}b$ relationship in the C23 phase, we obtain the two equivalent hexagonal axes $\mathbf{a}' = \mathbf{b}$ and $\mathbf{b}' = (\mathbf{c} - \mathbf{b})/2$. While this particular geometry is the most stable one for $V < 255$ bohr$^3$/molecule, it is not so for larger volumes. However, its higher symmetry allows us to calculate its energy curve for the whole volume range as a function of two parameters ($a'$ and $c'$) only, thereby enabling a complete characterization of the hexagonal phase ($r_{B8_b}$ curve in Fig. 1).

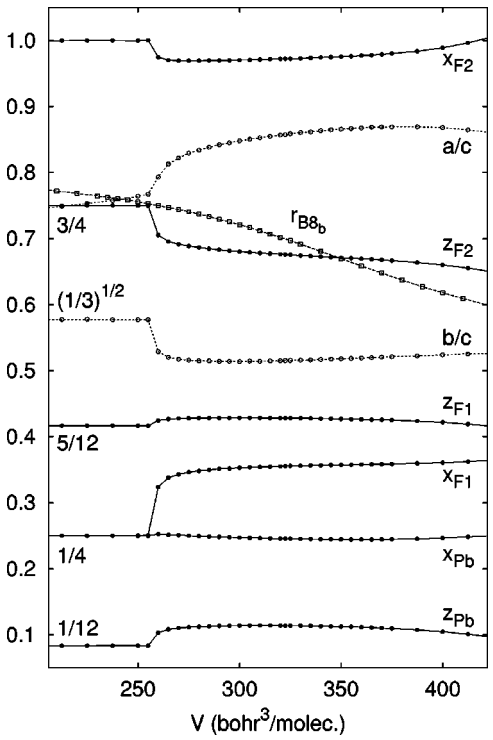


FIG. 1. Internal coordinates and lattice parameter ratios for the C23 phase, except $r_{B8_b}$, which is $a'/c'$ for the hexagonal $B8_b$ phase (corresponding to $b/a$ in the C23 phase).

We have also conducted the full optimization of the $P2_1/c$ monoclinic phase, which has 22 free parameters (i.e., positions of the six inequivalent ions, three cell edges, and $\beta$ angle). Note that the unit cell is doubled with respect to that of the C23 phase. Calculations were performed for volumes ranging from 230 to 280 bohr$^3$/molecule. We have used two different sets of starting configurations. The C23 phase (and thus also the $B8_b$ phase) can be described within the monoclinic structure using $\beta = 90°$ and $(a,c,2b)$ as lattice parameters, each ion giving rise to an $(x,z,y/2),(x,z,(1+y)/2)$ pair. Thus, we have started optimizations at monoclinic points corresponding to the minima of the C23 or $B8_b$ phases (depending on the volume). We have also used the experimental parameters for the monoclinic phase of the related $PbCl_2$ structure[9] as the starting point of a different set of optimizations. All of these 22 parameter optimizations converged to the corresponding C23 or $B8_b$ geometries, indicating that, at least in the neighborhood of these positions, there is no minimum of monoclinic symmetry. In order to obtain an approximate equation of state of the hypothetical monoclinic phase, we have therefore fixed the positions of the ions to the $PbCl_2$ values, optimizing only the three lattice parameters and $\beta$ angle. These are the results which we will present for the monoclinic phase.

Figure 2 shows the potential energy versus volume curves for the four phases of $PbF_2$ studied here. The lowest minimum is the one corresponding to the C1 cubic phase (empty squares), being the most stable structure in static (and also in ambient) conditions. The orthorhombic C23 phase (full circles) is very close in energy, having its minimum at a

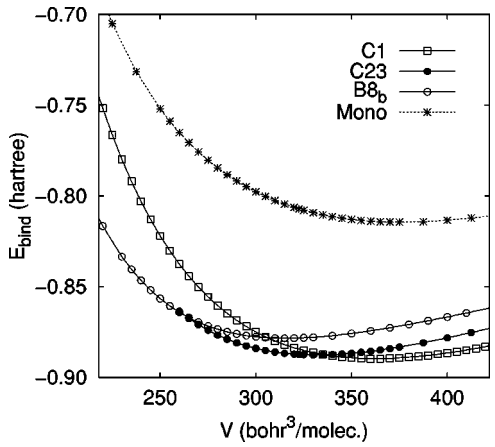


FIG. 2. Energy curves for the four phases of $PbF_2$ studied.

lower volume. On a further decrease of the volume, the C23 phase converges to the high-symmetry $B8_b$ hexagonal phase (open circles). The $B8_b$ phase has its minimum at an even lower volume than the C23 phase minimum, in a volume in which C23 is the most stable phase. Finally, the monoclinic phase with internal parameters fixed to their $PbCl_2$ values (stars) is predicted to be considerably higher in energy ($\simeq 3$ eV) than any other phase in this work.

In order to estimate the errors due to the lack of dipolar deformations in the *ai*PI wave function, we have computed *a posteriori* an empirical polarization energy correction using fixed polarizabilities of 1.49 and 2.43 $Å^3$ for the $F^-$ and $Pb^{+2}$ ions.[23] Given the high symmetry of the C1 and $B8_b$ phases, this correction only affects the C23 phase and the fixed-parameters monoclinic phase curves. The computed values of this correction are around $-0.003$ hartree for the C23 phase. Thus, it is expected that a rigorous calculation of the multipolar contributions to the energy curve will not affect significantly our results for this phase. If any, its effects are likely to lower the C1$\rightleftharpoons$C23 transition pressure slightly and increase the C23$\rightleftharpoons B8_b$ one. Although the polarization correction is larger ($\simeq -0.03$ hartree) for the fixed-parameters monoclinic phase, it is still insufficient to overcome the difference of 0.1 hartree with the cubic, orthorhombic, and hexagonal phases (Fig. 2).

The cell parameters of the zero-pressure static minima of the four phases are given in Table I, which also includes the available experimental data for the C1 and C23 phases. The calculated results show a very good agreement with the experimental data. Furthermore, the static bulk moduli calculated from the equation of state are 56.02, 57.87, 53.78, and 39.43 GPa for the C1, C23, $B8_b$, and monoclinic phases, respectively. These values compare well with the $B_0$ computed from elastic measurements in the C1 phase, 60.5, 55.9, and 60.3 GPa (see Ref. 24 and references therein), and also with the equation of state data of Ref. 4, 60.6 GPa for both C1 and C23 phases. Theoretical values given in Ref. 7, 71 GPa for C1 and 40 GPa for C23, are substantially different, probably due to a small number (10) and wide range (14.45–30.71 $cm^3$/mol) of volumes used in that work. The bulk modulus shows an appreciable change with pressure, being the computed $B_0'$ values 4.90, 4.98, 6.34, and 8.02 for each of the four phases. The molar volumes ($V_0$) of the phases are 32.32, 29.60, 28.18, and 33.53 $cm^3$/mol for C1, C23, $B8_b$, and monoclinic, respectively, showing that, upon increasing pressure, the transition sequence is expected to be C1$\rightarrow$C23$\rightarrow B8_b$. This also correlates with the respective coordinations of $Pb^{+2}$ of 8-fold, 9-fold (1+2+1 $F_1$ and 1+2+2 $F_2$), and 11-fold (3 $F_1$, 6 $F_2$, and 2 $F_1$) for the cubic, orthorhombic, and hexagonal phases. The data for the monoclinic phase with $PbCl_2$ internal parameters fall out of the range of the structural parameters of the other phases: it has an unrealistically low bulk modulus and high $B_0'$, computed at a higher $V_0$ relative to the other phases. Most probably, this is due to the restriction imposed on the internal parameters of this monoclinic structure during the optimization.

TABLE I. Optimized cell parameters and internal coordinates of the four phases, along with experimental data for the C1 and C23 phases (Ref. 5). All values are in atomic units.

| Phase | Cell parameters | Internal coordinates | | |
|---|---|---|---|---|
| Cubic | $a=11.31$ | | | |
| (Expt.) | $a=11.21$ | | | |
| Orthorhombic | $a=12.40$ | $Pb^{+2}$: | $x=0.245$, | $z=0.114$ |
| | $b=7.43$ | $F_1^-$: | $x=0.356$, | $z=0.428$ |
| | $c=14.40$ | $F_2^-$: | $x=0.973$, | $z=0.674$ |
| (Expt.) | $a=12.11$ | $Pb^{+2}$: | $x=0.244$, | $z=0.147$ |
| | $b=7.36$ | $F_1^-$: | $x=0.358$, | $z=0.415$ |
| | $c=14.45$ | $F_2^-$: | $x=0.949$, | $z=0.686$ |
| Hexagonal | $a'=8.015$ | | | |
| | $c'=11.35$ | | | |
| Monoclinic | $a''=22.23$ | | | |
| | $b''=7.305$ | | | |
| | $c''=18.49$ | | | |
| | $\beta=87.61$ | | | |

Table II contains the static transition data for $PbF_2$. The C1 phase is the most stable one at ambient pressure, and it changes to the C23 phase at 1.98 GPa. This is in reasonable agreement with the experiment (around 0.4 GPa at ambient temperature for the direct transition[4]), given the uncertainty in the calculations and the existence of hysteresis. We also predict the transition from the C23 to the $B8_b$ phase to occur at 20.2 GPa. It may be compared with the 14.7 GPa obtained from Raman spectra.[7]

The inclusion of thermal effects (both zero-point and finite-temperature) gives 300 K transition properties almost equal to the static ones (see Table II). The *P-T* phase equilibrium curves are depicted in Fig. 3. We also include in the phase diagram the hypothetical C1$\rightleftharpoons B8_b$ equilibrium curve, which falls completely within the C23 phase stability range. All the equilibrium lines are almost constant with tempera-

TABLE II. Static and ambient temperature transition pressures (in GPa) and volume changes (in $cm^3$/mol). The hypothetical cubic to hexagonal transition (in parentheses) is also included.

| | Static | | 300 K | |
|---|---|---|---|---|
| Transition | $P_{tr}$ | $\Delta V_{tr}$ | $P_{tr}$ | $\Delta V_{tr}$ |
| C1$\rightleftharpoons$C23 | 1.98 | −2.614 | 1.95 | −2.612 |
| (C1$\rightleftharpoons B8_b$) | 7.55 | −3.664 | 7.54 | −3.548 |
| C23$\rightleftharpoons B8_b$ | 20.15 | −0.898 | 21.64 | −0.789 |

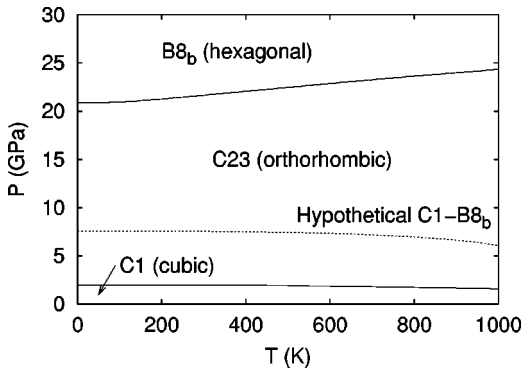


FIG. 3. Computed $P$-$T$ phase diagram of $PbF_2$.

ture, being very close to the static values. Both low pressure lines have slightly negative Clapeyron slopes, while the upper curve has a positive (and higher) Clapeyron slope. Given that all transitions proceed with decreasing volume, the entropy change is positive and small in going from the cubic to the orthorhombic phase, and is large and negative in going from the orthorhombic to the hexagonal phase. The calculated $\Delta S_{tr}$ values should be taken with caution, given the simple Debye model used here and the importance of Frenkel defects in the Clapeyron slope.[25]

## IV. SUMMARY

The results of *ai*PI calculations in $PbF_2$ support the existence of a post-cotunnite phase of hexagonal symmetry, with $Ni_2In$ ($B8_b$) structure. The other high-pressure candidate phase, the monoclinic post-cotunnite structure found in $PbCl_2$, is found to converge to the C23 and $B8_b$ structures when optimized. Additionally, the optimization of the monoclinic phase using the $PbCl_2$ internal parameters yields a high potential-energy surface. A full characterization of the equilibrium structures and equations of state of the phases involved is given here. It is expected to aid in the experimental determination of the post-cotunnite structure of $PbF_2$.

## ACKNOWLEDGMENTS

Thanks are due to Professor Mu Gu for helpful discussions. M.A.B. thanks the Spanish MEC for a grant. DGICyT Grant No. PB96-0559 is also acknowledged.

*Permanent address: Departamento de Química Física y Analítica, Universidad de Oviedo, 33006 Oviedo, Spain.

†Author to whom correspondence should be addressed. Permanent address: Departamento de Química Física y Analítica, Universidad de Oviedo, 33006 Oviedo, Spain. Electronic address: mblanco@mtu.edu

[1] S. E. Derenzo, W. W. Moses, J. L. Cahoon, R. C. C. Perera, and J. E. Litton, IEEE Trans. Nucl. Sci. **37**, 203 (1990).

[2] D. Z. Shen, G. H. Ren, Q. Deng, and Z. W. Yin, Sci. Sinica E **28**, 46 (1998).

[3] G. A. Samara, J. Phys. Chem. Solids **40**, 509 (1979).

[4] G. A. Samara, Phys. Rev. B **13**, 4529 (1976).

[5] R. W. G. Wyckoff, *Crystal Structures (Vol. II)* (Interscience, New York, 1960).

[6] H. Podsiadlo and J. Matuszewski, Mater. Chem. Phys. **37**, 397 (1994).

[7] H. E. Lorenzana, J. E. Klepeis, M. J. Lipp, W. J. Evans, H. B. Radousky, and M. van Schilfgaarde, Phys. Rev. B **56**, 543 (1997).

[8] J. Oberschmidt and D. Lazarus, Phys. Rev. B **21**, 2952 (1980).

[9] J. M. Léger, J. Haines, and A. Atouf, Phys. Rev. B **51**, 3902 (1995).

[10] J. M. Léger, J. Haines, and A. Atouf, J. Phys. Chem. Solids **57**, 7 (1996).

[11] J. M. Léger, J. Haines, A. Atouf, O. Schulte, and S. Hull, Phys. Rev. B **52**, 13 247 (1995).

[12] V. Luaña and L. Pueyo, Phys. Rev. B **41**, 3800 (1990).

[13] V. Luaña, A. Martín Pendás, J. M. Recio, E. Francisco, and M. Bermejo, Comput. Phys. Commun. **77**, 107 (1993).

[14] M. A. Blanco, V. Luaña, and A. Martín Pendás, Comput. Phys. Commun. **103**, 287 (1997).

[15] E. Francisco, A. Martín Pendás, and W. H. Adams, J. Chem. Phys. **97**, 6504 (1992).

[16] A. Martín Pendás, V. Luaña, J. M. Recio, M. Flórez, E. Francisco, M. A. Blanco, and L. N. Kantorovich, Phys. Rev. B **49**, 3066 (1994).

[17] J. M. Recio, M. A. Blanco, V. Luaña, R. Pandey, L. Gerward, and J. S. Olsen, Phys. Rev. B **58**, 8949 (1998).

[18] T. Koga, S. Watanabe, K. Kanayama, R. Yasuda, and A. J. Thakkar, J. Chem. Phys. **103**, 3000 (1995).

[19] T. Koga, K. Kanayama, S. Watanabe, T. Imai, and A. J. Thakkar (unpublished).

[20] C. Lee, W. Yang, and R. G. Parr, Phys. Rev. B **37**, 785 (1988).

[21] E. Francisco, J. M. Recio, M. A. Blanco, A. Martín Pendás, and A. Costales, J. Phys. Chem. A **102**, 1595 (1998).

[22] In all the optimizations at fixed volumes, all of the variables were included in the procedure except where explicitly noted. The optimum values for the previous volume were used as starting parameters in the C23 phase, allowing for a $10^{-7}$ hartree convergence to be achieved with about 170 energy evaluations. The 22-parameter monoclinic optimizations required $\simeq$1000 points, around 90 were needed in the three-parameter fixed-coordinates monoclinic calculations, and around 50 in the single-parameter $B8_b$ phase.

[23] H. Jiang, A. Costales, M. A. Blanco, M. Gu, R. Pandey, and J. D. Gale (unpublished). The dipole polarizabilities are fitted to the dielectric behavior of the C1 phase of $PbF_2$, within the context of shell-model calculations. A word of caution must be included here, since we have shown how hyperpolarizabilities play an important role in the defect structure.

[24] C. R. A. Catlow, J. D. Comins, F. A. Germano, R. T. Harley, and W. Hayes, J. Phys. C **11**, 3197 (1978).

[25] J. Oberschmidt, Phys. Rev. B **24**, 3584 (1981).